Bioorganic & Medicinal Chemistry 16 (2008) 10345–10355

Contents lists available at ScienceDirect

Bioorganic & Medicinal Chemistry

journal homepage: www.elsevier.com/locate/bmc

The role of molecular modeling in the design of analogues of the fungicidal natural products crocacins A and D

Patrick J. Crowley [a,*], Edward A. Berry [b], Thomas Cromartie [c], Fevzi Daldal [d], Christopher R. A. Godfrey [e], Dong-Woo Lee [d], Janet E. Phillips [a], Anne Taylor [a], Russell Viner [a]

[a] Syngenta, Jealott's Hill International Research Centre, Bracknell, Berkshire RG42 6EY, UK
[b] Upstate Medical University, 750 East Adams Street, Syracuse, NY 13210, USA
[c] Oncologic Inc., 626 Bancroft Way 3C, Berkeley, CA 94710-222, USA
[d] Department of Biology, Plant Science Institute, Johnson Research Foundation, University of Pennsylvania, Philadelphia, PA 19104, USA
[e] Syngenta Crop Protection Ag, Schaffhauserstrasse, CH-4332 Stein, Switzerland

ARTICLE INFO

Article history:
Received 29 February 2008
Revised 7 October 2008
Accepted 12 October 2008
Available online 17 October 2008

Keywords:
Crocacin
Respiration
Inhibitor
Fungicide
Modeling

ABSTRACT

Extensive molecular modeling based on crystallographic data was used to aid the design of synthetic analogues of the fungicidal naturally occurring respiration inhibitors crocacins A and D, and an inhibitor binding model to the mammalian cytochrome bc_1 complex was constructed. Simplified analogues were made which showed high activity in a mitochondrial beef heart respiration assay, and which were also active against certain plant pathogens in glasshouse tests. A crystal structure was obtained of an analogue of crocacin D bound to the chicken heart cytochrome bc_1 complex, which validated the binding model and which confirmed that the crocacins are a new class of inhibitor of the cytochrome bc_1 complex.

1. Introduction

The cytochrome bc_1 complex is an essential component of the cellular respiratory chain, which catalyses the electron transfer from quinol to cytochrome *c* and the translocation of protons across the inner membrane in mitochondria. Three subunits are essential for the electron transfer function: cytochrome *b*, cytochrome c_1 and the Rieske iron–sulfur protein (ISP). The roles of these redox centers are explained by the Q cycle hypothesis,[1] where there is a quinone reduction site near the negative side of the membrane (Q_i site) and a quinol oxidation site close to the positive side of the membrane (Q_o site).[2] The first electron of a quinol molecule at the Q_o site goes to the substrate cytochrome *c* via the ISP, and cytochrome c_1 in sequence, whereas the second electron passes sequentially to the cytochrome *b* heme ending up in a quinone/semiquinone radical at the Q_i site. In a complete Q cycle, two quinol molecules are consumed at the Q_o site and one molecule of quinol is regenerated while two protons are taken up on the negative side and four protons are released on the positive side of the membrane.

Inhibitors of the cytochrome bc_1 complex are of great interest, both as potential biologically active molecules, for example for controlling fungal diseases,[3,4] and also as tools for probing the structure and function of the proteins of the respiratory electron transport chain.[5] A number of inhibitors have been discovered during the last few years. These inhibitors can be divided into those acting on the Q_o site, and those acting on the Q_i site. Qi-site inhibitors include compounds such as antimycin **1**, and will not be considered further here.[6]

Q_o site inhibitors have been divided into further sub-classes based on their chemical structures, and their effects on the cytochrome *b* heme and the ISP. Three different classifications exist based mainly on (1) the position in the electron transfer chain where inhibition appears to occur (group I compounds inhibit reduction of the ISP, while Group II and stigmatellin inhibit between the ISP and cytochrome c_1[7]); (2) the position of the inhibitor in the Q_o site (compounds binding in the proximal niche or distal niche as revealed by crystallographic studies)[8,9] and (3) the effect of the inhibitor on mobility of the ISP, (compounds being classified as Pf or Pm inhibitors).[10,11] There is an imperfect correlation between inhibitors of the distal niche, whose binding site involves both cytochrome *b* and the ISP, inhibitors of electron transfer from the ISP to cytochrome c_1, and Pf inhibitors.

* Corresponding author. Tel.: +44 1344 414840; fax: +44 1344 413739.
E-mail addresses: patrick.crowley@syngenta.com, patrick.crowley@btinternet.com (P.J. Crowley).

0968-0896/$ - see front matter © 2008 Elsevier Ltd. All rights reserved.
doi:10.1016/j.bmc.2008.10.030

Pf inhibitors fix the Rieske ISP head group, while Pm inhibitors mobilize it, and each bind to a different site within the Q_o pocket of cytochrome *b*. Inhibitors shown in Figure 1, such as stigmatellin **2** and 5-undecyl-6-hydroxy-4,7-dioxobenzothiazole (UHDBT) **3**, block electron transfer from the ISP to cytochrome *c* and belong to the Pf class, binding in the distal niche. The β-methoxyacrylates such as myxothiazole **5**, methoxyacrylate stilbene **6**, and azoxystrobin **7**, which block electron transfer from quinol to the ISP, belong to the Pm class and bind in the proximal niche.

The differences between Pf and Pm inhibitors are shown in the two pictures in Figure 2, where the inhibitors stigmatellin **2** and azoxystrobin **7** both stack against the proline in the PEWY motif in the backbone. In the left hand picture in Figure 2, azoxystrobin **7** extends downwards and makes a direct H-bond with the backbone N of the PEWY glutamate, but does not interact with the ISP. In the right hand picture, stigmatellin **2** extends upward and fixes the ISP by hydrogen bonding to the histidine. It makes an indirect H-bond to N of the PEWY glutamate, bridged by the PEWY carboxylate. Famoxadone **4** is intriguing because although it blocks electron transfer from the ISP to cytochrome *c*, it binds in the proximal niche and in many ways resembles the Pm inhibitors.

In 1994 Höfle and Reichenbach at GBF in Braunschweig, Germany isolated the new compounds crocacins A, B, C and D from the myxobacterium *Chondromyces crocatus* (3), and identified their structures as the novel *Z*-enamides[12] **8–11**, shown in Figure 3. Höfle and Reichenbach showed that crocacins A and D inhibited the electron transport chain at complex III in a beef heart mitochondrial respiration assay, and that they inhibited the growth of several fungi in vitro. The acid crocacin B, and the amide lacking the Z-enamide, crocacin C, were reported not to be active.

Certain inhibitors of cytochrome bc_1 complex, such as azoxystrobin **7** are extremely important agricultural fungicides due to their high potency and control of a broad spectrum of plant pathogens.[13,14] Since the crocacins are novel compounds that are good inhibitors of the electron transport chain at the cytochrome bc_1 complex, and that also show evidence of fungicidal activity, we became interested in them as leads for new agricultural fungicides.

Höfle and Reichenbach very kindly provided us with samples of crocacins A and D, and we confirmed their activity against mito-

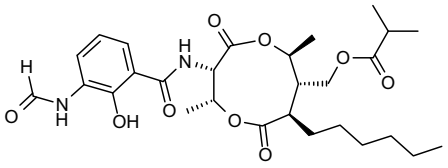

1 Antimycin

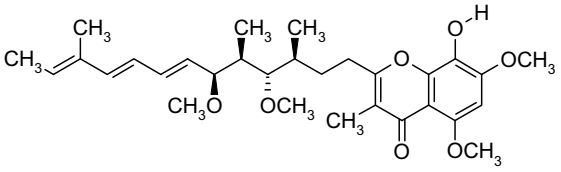

2 Stigmatellin

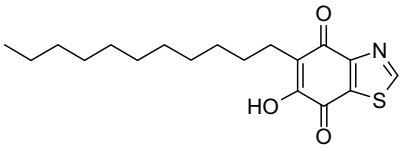

3 UHDBT

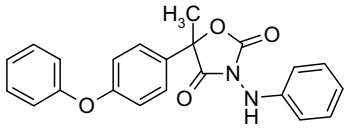

4 Famoxadone

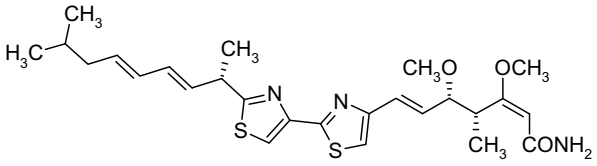

5 Myxothiazole

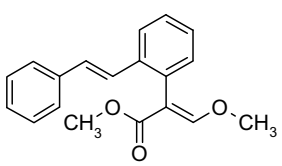

6 Methoxyacrylate Stilbene

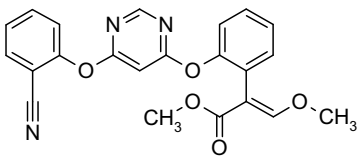

7 Azoxystrobin

Figure 1. Mitochondrial respiration inhibitors.

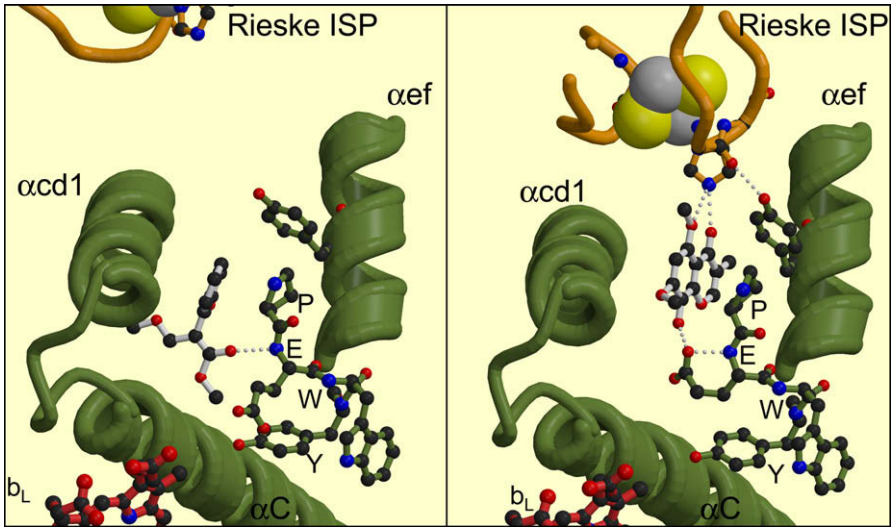

Figure 2. Comparison of the binding mode of azoxystrobin **7**, a Pm inhibitor (left) and stigmatellin **2**, a Pf inhibitor (right) relative to the "PEWY" proline and the acd1 helix. The figures are seen in the same orientation after the structures were superimposed based on the rigid transmembrane helices. The figures are based on unpublished structures (E.A. Berry) of the inhibitors bound to chicken cytochrome bc_1.

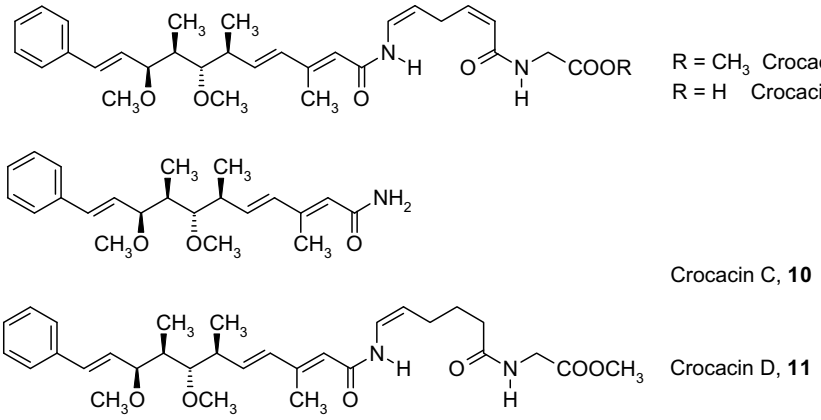

Figure 3. Structures of crocacins A–D.

chondrial respiration at the cytochrome bc_1 complex in a beef heart NADH oxidase assay with crocacin D **11** being slightly more active than crocacin A **8**. We also found that they showed activity by foliar spray against *Blumeria graminis f. sp. tritici* (wheat powdery mildew), *Mycosphaerella graminicola*, (*Septoria tritici*, wheat glume blotch), *Phytophthora infestans* (potato late blight), *Plasmopara viticola* (vine downy mildew), *Puccinia triticina* (wheat brown rust), on plants (Table 1). Interestingly, although stigmatellin **2** was quite active in mitochondrial NADH oxidase assays, for example from beef heart, it showed very little fungicidal activity on plants.

An added interest in crocacin A **8** was that it showed little or no cross-resistance to a strobilurin resistant strain of *Plasmopara viticola* in small vine plants in the glasshouse, or against a strain of yeast that had been engineered with the G143A mutation responsible for fungicide resistance.[15]

Although the natural crocacins have interesting biological activity, their physical properties are sub-optimal for agricultural use in the field, especially their stability. In simulated sunlight tests in the laboratory, using thin films on glass slides in order to predict stability under field conditions, crocacins A **8** and D **11** had very poor photostability, with 50% of parent compound being lost in 7 and 37

Table 1
Activity of inhibitors of the cytochrome bc_1 complex.

Compound	Inhibitor	Wheat Powdery Mildew	Wheat Glume Blotch	Potato Late Blight	Vine Downy Mildew	Wheat Brown Rust	NADH oxidase IC_{50} (nM)
Breakpoint[a] *(μM)*							
8	Crocacin A	>180[b]	>180	>180	45	45	56
11	Crocacin D	>180	45	45	45-9	9	36
2	Stigmatellin	>180	>180	>180	180	>180	81
7	Azoxystrobin	<1.8[c]	<1.8	<1.8	<1.8	<1.8	120

[a] breakpoint is the lowest concentration at which control of disease was 100%
[b] > indicates that the compound was not active at the highest concentration tested.
[c] < indicates that the compound was 100% active at this concentration but was not tested at lower concertrations.

minutes respectively.[16] These properties would severely limit their practical use, and would have to be addressed in a programme of chemistry to find useful analogues.

In this paper we report modeling and structure activity studies on this new class of mitochondrial respiration inhibitors.

2. Results and discussion

2.1. Development of a binding model

The structural complexity of the naturally occurring crocacins prohibits their use as commercial agrochemicals. We therefore wanted to understand how they might bind to the active site, in order to help us design synthetic analogues that were both more active and structurally simpler, and we embarked on a study on their conformation and the development of a binding model.

Although there are no crystal structures of the mitochondrial cytochrome bc_1 complexes from agricultural fungal pathogens, several structures from beef, chicken and yeast are available.[17–20] As a result, there is detailed information about interactions between cytochrome bc_1 and a number of Q_o inhibitors such as stigmatellin **2**, famoxadone **4** and azoxystrobin **7**.[10,11] In order to check the relevance of these crystal structures for our purposes, we looked at the sequence homology between cytochrome *b* sequences from beef, chicken, yeast and three agriculturally important plant-pathogenic fungi (wheat brown rust, wheat glume blotch and wheat powdery mildew). Although the percent sequence identity between the beef and chicken cytochrome *b* sequences and the three fungal sequences was only between 48.2% and 57.5%, there was very high homology of the residues around the active site. Twenty-four residues are within 4 Å of the three Q_o site ligands in the protein structures 1sqx[5], 1sqp[5] and 1sqq[5], and this was used to define the Q_o site residues. Of these 24 residues, 15 are identically conserved between the beef, yeast and three fungal sequences. For the remaining nine residues, the changes are very conservative (see Table 2).

In all cases except one, the change is from a hydrophobic residue to another hydrophobic residue of a similar size. The exception is Lys269, present in both the mammalian sequences, but the lysine side chain points *away* from the Q_o site, and only its backbone atoms are in contact with the Q_o site ligands so the nature of the side chain is not likely to be critical. Because of the similarities of the Q_o sites and in order to maintain consistency with our in vitro assay (based on beef heart mitochondria) we felt that the beef structure was a reasonable one to use as a model. Additionally, experience in previous work with the strobilurins[13,14] gave us confidence that the beef heart assay correlated reasonably well with antifungal activity when dealing with complex III inhibitors.

The crocacins have a complex side chain containing four contiguous chiral centres and an identical fragment is found in stigmatellin. In developing a binding model for the crocacins we therefore paid particular attention to the mode of binding of stigmatellin, despite its poor activity as a fungicide *in planta*.

The crystal structure of stigmatellin **2** bound to the bovine mitochondrial cytochrome bc_1 complex (1sqx) showed that it makes two hydrogen bonding interactions, one between the carbonyl group of stigmatellin and the Nε of His161 in the ISP, which gives rise to the Pf classification as previously described, and a second between the phenolic hydroxyl of stigmatellin and the carboxyl group of Glu271. Glu271 also hydrogen bonds its own backbone nitrogen, so the carboxylate oxygen can be seen as mediating a bond between the inhibitor and the Glu271 nitrogen.

With the similarity of their side chains, it seemed plausible that the crocacins might bind in a similar manner to stigmatellin, with the *Z*-enamide and ester groups as the key hydrogen bonding groups. However, in our initial docking studies it proved difficult to dock the crocacins into the Q_o site of the 1sqx structure due to lack of space. The crystal structures of two other Q_o site inhibitors, myxothiazole **5** (1sqp) and methoxyacrylate stilbene **6** (1sqq) bound to the bovine *bc1* complex were also available. These inhibitors both belong to the methoxyacrylate (MOA) class and show an alternative conformation of the Glu271 residue, in which its side chain is directed out of the active site. This creates more space in the Q_o site, and also makes the backbone nitrogen of Glu271 available for hydrogen bonding. Both myxothiazole **5** and methoxyacrylate stilbene **6** take advantage of this, and form hydrogen bonds with this nitrogen (Fig. 4). We therefore investigated the possibility that the crocacins also bind directly to the backbone nitrogen of Glu271 (like the MOA inhibitors) with the side chain of this residue in the out-of-pocket alternative conformation. It has been suggested that the catalytic cycle involves movement of Glu271,[18,21]

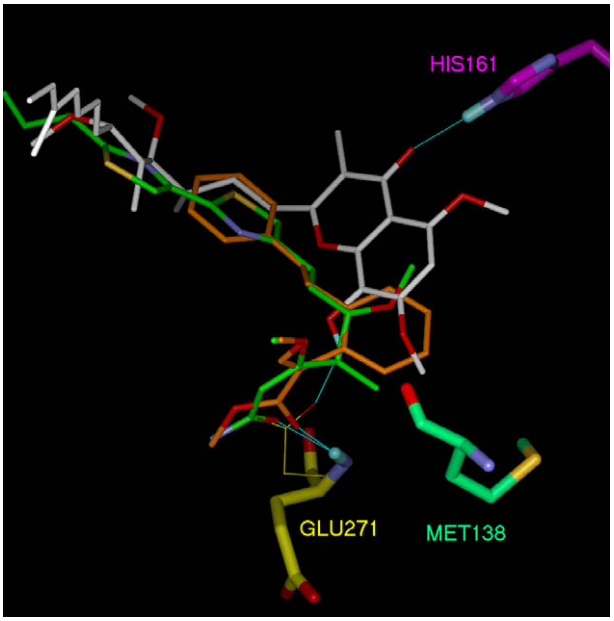

Figure 4. Superposition of the binding modes of stigmatellin **2** (white carbons), myxothiazole **5** (green carbons) and methoxyacrylate stilbene **6** (orange carbons) from the PDB structures 1sqx, 1sqp and 1sqq, respectively. Glu271 is shown in both the Pf conformation (1sqx, thin bonds) and the Pm conformation (1sqq, thick bonds). Hydrogen bonding interactions are shown in thin blue lines.

Table 2
Alignment of sequences; the nine variable residues around the cytochrome *b* Q_o site.

Numbering (beef)	121	124	125	129	164	269	274	294	298
Beef	L	M	A	M	I	K	F	L	I
Chicken	L	M	A	V	A	K	F	L	V
Wheat brown rust	I	I	A	M	I	V	L	M	L
Wheat glume Blotch	V	M	A	L	V	V	L	M	I
Wheat powdery Mildew	I	I	V	L	L	V	L	M	I
Yeast	I	I	A	L	L	V	L	M	I

and it may be that the stigmatellin complex mimics an intermediate state in which Glu271 binds the substrate.

The docking program GOLD[22] was used to dock crocacin A **8** into the Q_o site with the Glu271 side chain in the out-of-pocket conformation. Crocacin A **8** was used rather than crocacin D **10** because it has one fewer rotatable bond (reducing the complexity of the docking problem) but is of comparable potency. GOLD was run using a range of different program settings, to generate 100 or so feasible docking solutions, with very similar GOLD scores. The fact that GOLD was not able to identify a single docking solution is not greatly surprising; crocacin A **8** contains 13 rotatable bonds and its great flexibility represents a formidable task for any docking software. Also, GOLD works by using a genetic algorithm that explores a population of diverse docking solutions from a population of randomly generated initial trial solutions.

In order to select a preferred docking solution from those generated by GOLD, we performed a conformational analysis of crocacin A **8** to identify those solutions with the lowest internal conformational energies. The allowed and/or preferred rotameric states of each of the 13 rotatable bonds were determined by a combination of two methods: (i) conformational searching performed on model compounds with molecular mechanics methods; and (ii) by searching the Cambridge Structural Database[23] for molecules containing similar molecular fragments to those found in crocacin A **8**. The results are summarized in Table 3. The preferred dihedral values for rotatable bonds t1 and t2 (close to +120°/−120° or −120°/+120°, respectively) are those that allow an internal hydrogen bond between the two amide groups in crocacin A **8**, resulting in a 'hairpin' conformation in this region of the molecule. Further along the molecule, the four contiguous chiral centres were found to add rigidity to their region of the side chain; a single conformation was found for rotatable bonds t9–t12, the same conformation as that reported in an earlier NMR study.[24]

The conformational analysis enabled us to select one of the GOLD docking solutions as our binding model. This model was further refined by 'relaxing' the bound ligand and the surrounding residues within 6 Å using a molecular mechanics method.[25] The GOLD program works by considering the binding site as rigid, and the effect of this relaxation step was to allow minor movements to occur so as to alleviate any slight steric clashes caused by this approximation. The final binding model is shown in Figure 5, but the salient features are as follows: (i) the side chain fragment containing the four contiguous chiral centres binds in the same conformation and position as the equivalent fragment of stigmatellin **2**; (ii) the *Z*-enamide carbonyl of crocacin A **8** accepts a hydrogen bond from the Nε of His161 in the ISP, in a similar manner to the carbonyl group of stigmatellin **2**; (iii) the *Z*-enamide linking group of crocacin A **8** adopts a hairpin conformation allowing an intramolecular hydrogen bond between the two amide groups; (iv) the glycine nitrogen of crocacin A **8** donates a hydrogen bond to the carbonyl group of Met138; and (v) the glycine ester oxygen of crocacin A **8** accepts a hydrogen bond from the backbone nitrogen of Glu271, in a similar manner to the myxothiazole **5** and methoxyacrylate stilbene **6** ligands.

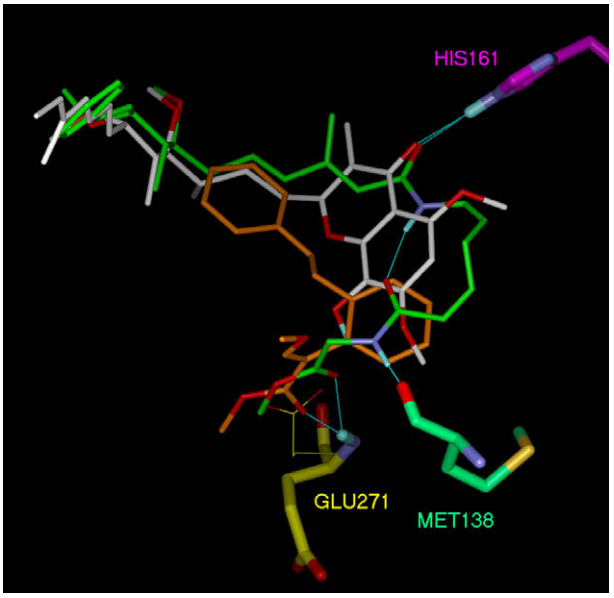

Figure 5. Superposition of the proposed binding mode of crocacin A **8** (green carbons) on that of stigmatellin **2** (white carbons) and methoxyacrylate stilbene **6** (orange carbons). Hydrogen bonding interactions are shown in thin blue lines.

The proposed binding mode for the crocacins therefore combines some of the features of the binding of stigmatellin **1** and some of the binding features of myxothiazole **5** and methoxyacrylate stilbene **6**. The differences in binding between the crocacins and methoxyacrylate stilbene could explain the apparent lack of cross-resistance of the crocacins to the strobilurins.

2.2. Design of analogues of crocacins A and D—Additional considerations

As mentioned previously, as well as optimizing fungicidal activity, it was necessary to address the poor photostability of the crocacins (see Table 4). Our experiments showed that both crocacins A and D were rapidly degraded by simulated sunlight, and that none of the large number of products could be identified, or had any biological activity. Common reactions of double bonds in the presence of light are rapid *E*/*Z* isomerisation, and oxidation to give allylic hydroperoxides in the presence of oxygen, to give products which can then degrade to a multiplicity of further products. In a number of classes of agrochemicals, for example the pyrethroids and the

Table 3
Rotatable bonds used in the conformational analysis of crocacin A 8.

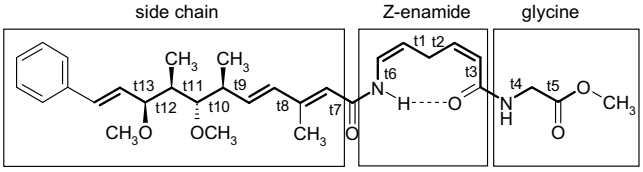

Dihedral angle (°)[a]	Preferred values[b]	Docked[c]	Jansen et al.[d]	1sqx[e]
t1	±120	107.3		
t2	±120	−108.3		
t3	180	−143.9		
t4	±90or180	94.5		
t5	0 or 180	151.6		
t6	180	158.8		
t7	180	152.6		
t8	180	−171.5		
t9	±120	139.2	−120	−171.9
t10	−60	−70.2	−60	−75.6
t11	180	173.9	180	174
t12	180	−171.6	180	169.1
t13	−90	−112.8	−60	131.2

[a] Ester bonds were assumed to be trans.
[b] The preferred rotamers for these bonds, as determined by conformational analysis and Cambridge Structural Database[23] (CSD) searches.
[c] The dihedral angles exhibited in the final binding model of crocacin A.
[d] The dihedral angles determined by NMR[24].
[e] The dihedral angles for the equivalent bonds of stigmatellin **2** in the 1sqx structure.

Table 4
Activity of side chain analogues on NADH oxidase and vine downy mildew on plants.

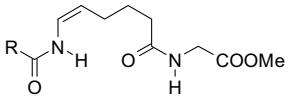

No.	Side chain R	IC_{50} NADH Oxidase (nM)	Breakpoint vine downy mildew (μM)	T_{50} glass slides (h)
11	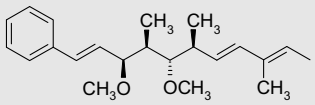	36	25	0.6
12	n-$C_{12}H_{21}$-	24	>100	0.1
13	n-$C_6H_{11}O$- 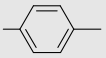	21	>100	5
14	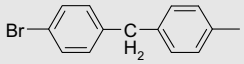	17	10	12
15	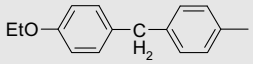	9	25	20
16	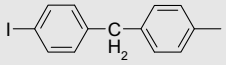	18	10	NT
17	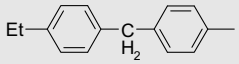	16	10	NT

NT, not tested.

strobilurins[13,26], the presence of double bonds has been shown to give rise to significant instability to sunlight, and replacement or modification of these groups led to much greater robustness in performance in the field. It therefore seemed likely that the lipophilic side chain of the crocacins with its array of three double bonds and the *Z*-enamide, were responsible for their lack of photostability. As part of the design process therefore, it was deemed essential to investigate the replacement of these groups with stable functionalities, such as aromatic groups, a strategy that had met with success in the development of stable analogues of the strobilurins.[13] We also believed that it would be desirable, and probably necessary, to find a more stable linking group to replace the potentially unstable *Z*-enamide.

To assess the activity of compounds synthesized in our analogue programme we needed a measure of intrinsic fungicidal activity as well as activity on whole plants. We therefore decided to use a mitochondrial NADH oxidase assay for the intrinsic activity. Because mitochondria from agriculturally relevant fungal sources are not generally available, we used a beef heart mitochondrial NADH oxidase assay, which had proved to be a sensitive and a reasonable indicator for activity in fungi in previous work,[13] and we used this screen as the first line assay in our cascade for testing crocacin analogues. In limited studies, we showed that results from an NADH oxidase assay using mitochondria from the fungus *Neurospora crassa* correlated well with results from using mitochondria from beef heart, which confirmed that our choice of assay was reasonable.

It should be noted that the NADH oxidase assay cannot discriminate between inhibition of NADH dehydrogenase (complex I) and the cytochrome bc_1 complex (complex III). A small range of compounds were tested in a succinate oxidase assay, which detects activity on either succinate dehydrogenase (complex II) or the cytochrome bc_1 complex, and activity exactly correlated with that on the NADH oxidase assay.

2.3. Replacement of the side chain

Despite the ultimate likely requirement for replacement of all the double bonds in the crocacin structure, we decided to maintain the *Z*-enamide in our first analogues, as we believed that finding suitable replacements for the side chain would be easier than for the *Z*-enamide group. As crocacin D **11** was more active than crocacin A **8**, and has only one *Z*-double bond, we decided to concentrate on first replacing the complex side chain of crocacin D **11** with simpler groups.

In our first analogues, we replaced the whole the side chain with simple n-alkyl chains.[27,28] We were gratified to find that certain analogues, for example, **12** (Table 4), were very active in the beef heart mitochondrial respiration assay but unfortunately showed no fungicidal activity.

We then decided to explore replacing the *n*-alkyl chain with side chains containing benzene rings, which we hoped would be better mimics of the unsaturated side chain in the natural products, and would be more photostable. We began by synthesizing compounds with a benzamide moiety, and modeling various benzamide side chains substituted in the 3- and 4-positions showed that 4-substituted benzamides provided a good fit in the active site. Our first analogues contained an *n*-alkoxy-benzamide, as in **13**, which showed very good activity on the NADH oxidase assay, but were inactive as fungicides. Further modeling showed that substituting the benzamide with a 4-substituted benzyl group gave a very good overlay with the crocacin side chain (Fig. 6). Indeed this proved to be the case, with compounds **14**–**17** showing not only potent inhibition of respiration, but also activity on vine downy mildew on small vine plants at a level similar to or better than the crocacins. Figure 6 shows the excellent overlay of the compound **17** with crocacin A **8**.

The relationship between structure and photostability was not straightforward. When the conjugated diene was replaced by a

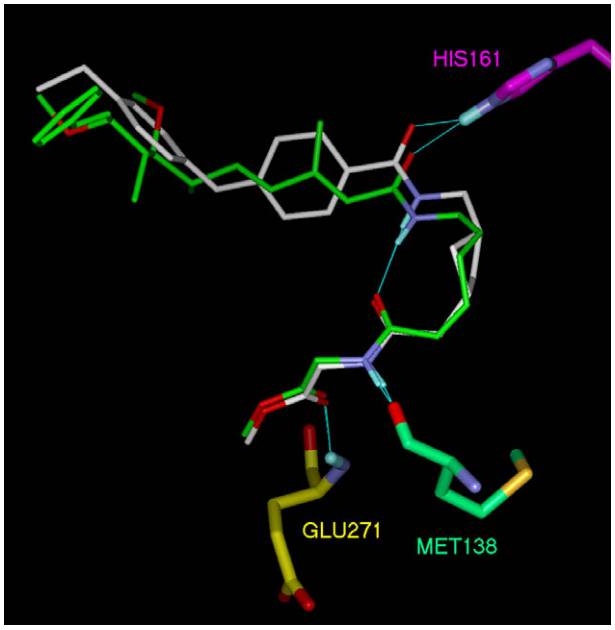

Figure 6. Superposition of compound **17** (white carbon atoms) on crocacin A **8** (green carbon atoms). The thin blue lines represent putative hydrogen bonds.

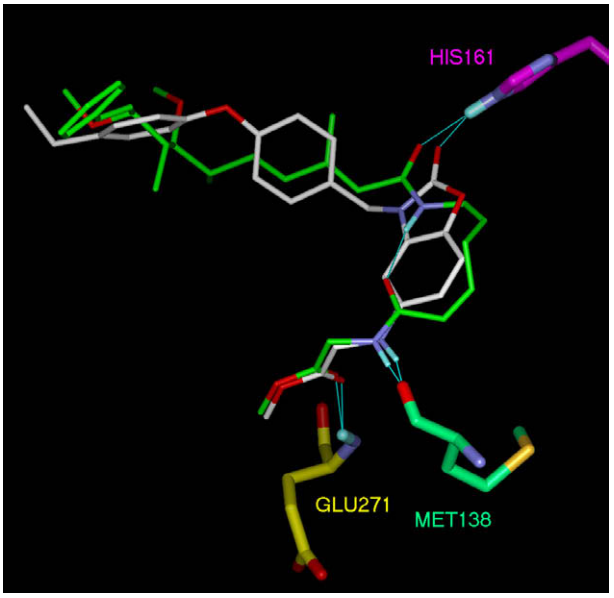

Figure 7. Superposition of crocacin A **8** (green carbon atoms) on benzoxazolidinone **21** (white carbon atoms). The thin blue lines represent putative hydrogen bonds.

phenyl group, as in compounds **14** and **15**, the hoped for greater photostability than the natural product was indeed found. However, when the conjugated diene was replaced with an alkyl chain, as in **12,** photostability was unexpectedly reduced.

2.4. Replacement of the *Z*-enamide

Having found very promising synthetic alternatives for the side chains of crocacin A and D, we turned our attention to finding more stable synthetic replacements for the *Z*-enamide.

We decided to explore very rigid structures, where the entire hydrogen bonding motif present in crocacins A **8** and D **11**, consisting of the enamide and the glycine amide and the chain between them, was replaced by a heterocycle such as the benzoxazolidinone ring system as in **18**–**21**. The first compound modeled was **21** (Fig. 7) which gave a convincing overlay, where the hydrogen bond to His161 of the ISP was provided by the oxazolidinone carbonyl group, the hydrogen bond to Glu271 came from the ester carbonyl, and a third hydrogen bond, to Met138, was donated by an aniline NH holding the ester side chain. Despite an apparently good overlay, this compound was inactive in the NADH oxidase assay. However, compounds **18** and **19**, with the aniline NH replaced by an oxygen, which retained the crucial hydrogen bonds to His161 and Glu271 but lacked the postulated hydrogen bond to Met138, showed more promising IC_{50}'s of 45 and 75 nM, respectively. Disappointingly, compounds **18** and **19** showed no activity on vine downy mildew on plants, which may be due to a still insufficient enough level of intrinsic activity.

As well as trying relatively rigid linking groups, we explored using very flexible chains to replace the enamide, hoping that this flexibility would allow the molecule to find a suitable conformation. We made several analogues with simple alkyl chains, with or without an oxygen atom, such as **22** and **23**. Both compounds modeled well, as expected, but were only weak inhibitors, with IC_{50}'s of 230 and 400 nM, respectively.

Finally, we tried an approach where just the *cis*-double bond in the *Z*-enamide linker of crocacin D **11**was replaced. A *cis*-cyclopropane seemed a suitable isosteric replacement, so we synthesized compound **24**, which modeled well. However, **24** was only very weakly active on the NADH oxidase assay (see Table 5). Another approach that had been employed with the β-methoxyacrylates, was incorporation of the *cis*-double bond into a benzene ring,[27] as in **25**, but this type of analogue was completely inactive. This was consistent with our model, which shows that there is no space for an additional ring.

2.5. Crystal structure

Unfortunately insufficient sample of crocacin A or D was available for a crystallographic study. However, a crystal structure was obtained for the 4-iodobenzyl analogue **16** bound at the active site of the chicken heart cytochrome bc_1. The compound was soaked into the cytochrome bc_1 complex, which had been purified from chicken hearts and then crystallized with no added inhibitors. These crystals are known to have the ISP in the "cytochrome c_1" position[19] complex. Diffraction datasets were collected at wavelengths of 1.7414, 1.2398 and 0.9202. The structure has been submitted to the Protein Data Bank as PDB ID 3cwb.

Although the resolution of 3.4 Å does not allow precise atomic model-building, the iodine atom of **16** was unambiguously located near the quinol reaction (Q_p) site by the high electron density and anomalous scattering. The location of the iodine atom, and the extended shape of the electron density allowed relatively unambiguous placement of compound **16** through the region where both stigmatellin and the strobilurins bind (Fig. 8). It was clear that in the structure the ISP has moved down to become part of the centre Q_p binding site, that is, in the cytochrome *b* position, which was most likely caused by a hydrogen bond from the inhibitor benzamide carbonyl to the His161 NH of the ISP, as seen in stigmatellin. In the refined structure, the position of the ISP is identical within error to that in the presence of stigmatellin: after superposition based on the rigid transmembrane helices, the position of the Fe_2 atom of the cluster differed by 0.36 and 0.41 Å from that in two stigmatellin-containing structures from chicken (2bcc[19] and 3bcc[19]) and 0.63 Å from that in the bovine structure (1sqx). Comparing Cα atoms of residues 74–196 in the ISP gave average deviations of 0.48, 0.66, and 0.94 Å and rotation angles of 1.0°, 1.4°, and 2.6° with the same three structures, again superimposed based on the transmembrane helices of cytochrome *b*. The hydrogen bond is

Table 5
Activity of *Z*-enamide analogues on NADH oxidase.

No.	Structure	IC_{50} (nM), NADH oxidase
18	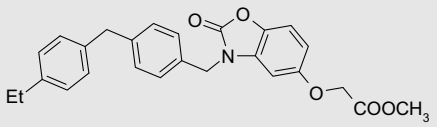	45
19	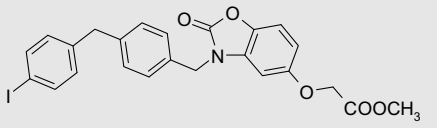	75
20	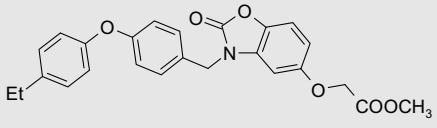	140
21	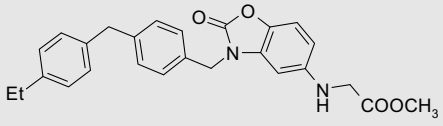	Inactive
22	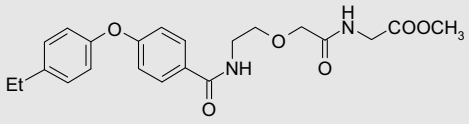	230
23	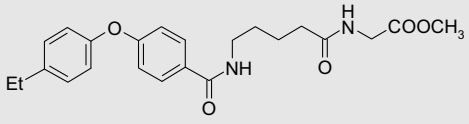	400
24	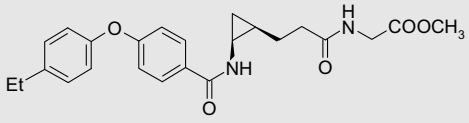	900
25	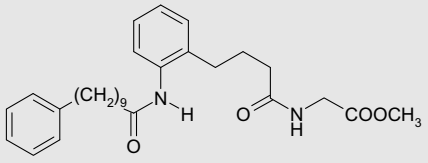	Inactive

clearly defined in the electron density. In contrast, famoxadone and fenamidone, which do not form a proposed hydrogen bond to His161 of the ISP, maintain the ISP in a significantly different fixed position, rotated about 10° and with Fe_2 displaced 1.3–1.8 Å from that of the structure containing stigmatellin (1sqx). There is also strong support from the electron density for the hydrogen bond between the ester carbonyl of **16** and the amide NH of residue Glu271 (Glu272, chicken) in the PEWY stretch of the protein backbone, as proposed from the modelling. The structure also supports the proposed intramolecular hydrogen bond between the enamide carbonyl group and the glycine amide NH of **16**. Although it is not possible to rule it out, the electron density does not support a hydrogen bond from the glycine NH of the inhibitor to the carbonyl O of Met138 (Met139, chicken). This could explain the inactivity of analogue **21**, although it is possible that the overall interaction is unfavourable due to other effects, such as the NH desolvation penalty[29] or protein conformational strain. However, the fact that compounds **19** and **20**, which are incapable of forming this bond, have much higher activity than **20** in the NADH oxidase assay, make it likely that this hydrogen bond is not formed.

Cocrystallization of **16** or **19** with the bovine heart cytochrome bc_1 complex was attempted under conditions that sometimes produce diffraction quality crystals in the presence of stigmatellin. No crystals were obtained with either inhibitor, and it seemed unlikely that soaking the inhibitors in would be effective in crystals with tightly bound stigmatellin occupying the Q_o site.

The photosynthetic bacterium *Rhodobacter capsulatus* has a cytochrome bc_1 complex with subunits homologous to the three core subunits of the mitochondrial bc_1 complex. Figure 9 shows the electron paramagnetic resonance (EPR) spectra of chromatophores with different inhibitors or endogenous ubiquinone at the Q_o site under conditions for observing the spectrum of the reduced Rieske Fe_2S_2 cluster, and Table 6 gives the g values. Cells were grown in respiratory conditions and prepared in air-oxidized conditions, with samples of final concentration of 100 μM inhibitor and 5 mM ascorbate. With endogenous ubiquinone (no inhibitor) there is a relatively sharp g_x transition at 1.809. This peak remains sharp but is shifted to 1.782 in the presence of stigmatellin **2**, which, along with presumably ubiquinone, forms a hydrogen bond with the ISP ligand His161 (His156 in *R. capsulatus*) which results in the cytochrome *b* position of the ISP extrinsic domain. In the presence of myxothiazole **4** the g_x peak is greatly broadened and diminished in amplitude. From crystal structures it is known that the ISP extrinsic domain is in the cytochrome c_1 endogenous ubiquinone and thus eliminates its hydrogen bond with His161, while myxothiazole itself has no atom positioned to form such a bond. Thus there is a correlation between the sharp g_x signal, formation of the hydrogen bond with His161, and the cytochrome *b* position of the ISP.[30] The fact that the iodo crocacin analogue **16** also results in a sharp g_x band, at $g = 1.808$, close to that of stigmatellin, provides further evidence confirming the modeled hydrogen bond between the crocacins and the ISP ligand His161. The lack of a shift in g_x for **19** was consistent with its much poorer activity in the NADH oxidase assay than **16,** and also with its inability to form crystals with the chicken heart cytochrome bc_1 complex.

A comparison between the modeled binding mode of crocacin A and the crystallographically determined binding mode of iodo analogue **16** is shown in Figure 10. This shows the generally very good agreement between the two structures and confirms the validity of using the modeled structure for design of crocacin analogues. The only significant difference was that the observed conformations of Glu271 and Met138 (thin bonds) are slightly different to those of the modeled structure (thick bonds), which further helps to explain the lack of a hydrogen bond from the crocacin amide NH to Met138.

3. Conclusions

In conclusion, a binding site model of crocacins A and D was developed which was consistent with X-ray crystallographic analysis of an analogue bound to the chicken heart cytochrome bc_1 complex. The mode of binding is significant in sharing features of both the methoxyacrylate inhibitors and stigmatellin. One classification of inhibitors separates them into (1) proximal-niche inhibitors like the methoxyacrylate family, which interact directly with the backbone nitrogen of the PEWY Glu271 (bovine) but which do not extend upwards to interact with the ISP, and (2) distal-niche inhibitors such as stigmatellin, the alkyl hydroxynapthoquinones, and alkyl hydroxybenzothiazoles, which extend upwards and fix the ISP by H-bonding to the histidine, and H-bond indirectly to the PEWY backbone. The crocacins would appear to be inhibitors which occupy both sites simultaneously.

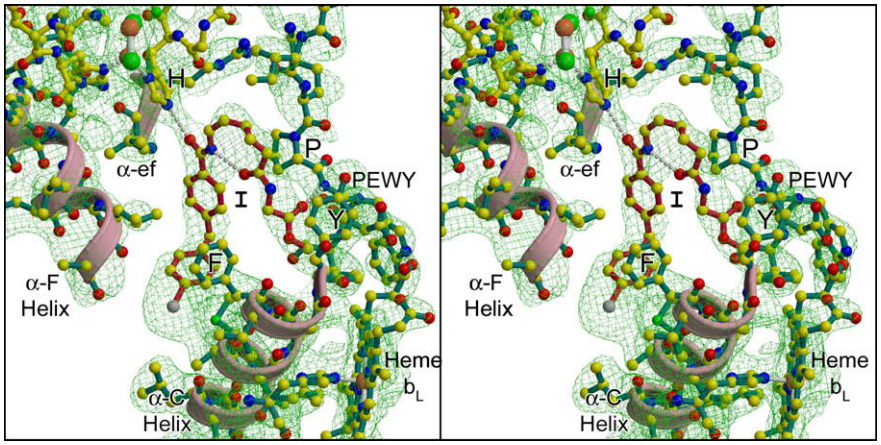

Figure 8. X-ray Structure of iodo analogue **16** (crimson bonds, yellow carbons) bound to the Q_o site of chicken cytochrome bc_1 complex, shown in stereo view. H is His161 of the iron–sulfur protein (yellow bonds); I is the centre of iodo analogue **16**; PEWY is the sequence from the conserved Glu271 (P) stretch of cytochrome *b* to the tyrosine (Y); F is Tyr129 leading from the α-C helix. Helices α-C, and α-ef are indicated by salmon colored ribbons.

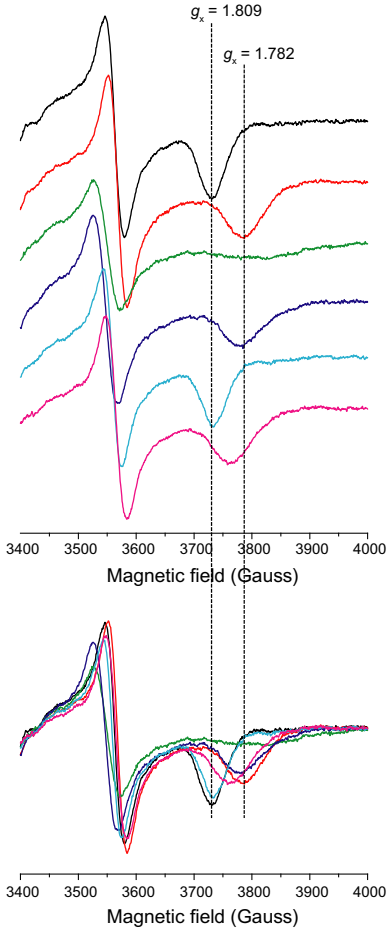

Figure 9. EPR spectra of the $[Fe_2S_2]$ cluster of ISP of *R. capsulatus* chromatophore membranes with inhibitors of mitochondrial respiration. Key: no inhibitor —, stigmatellin —, myxothiazole —, famoxadone —, compound **19** —, compound **16** —.

Table 6
G values for EPR spectra of inhibitors

Inhibitor	g_y	g_x
No inhibitor	1.895	1.809
Stigmatellin	1.891	1.782
Myxothiazole	1.901	1.771
Famoxadone	1.903	1.786
Compound **19**	1.897	1.808
Compound **16**	1.893	1.793

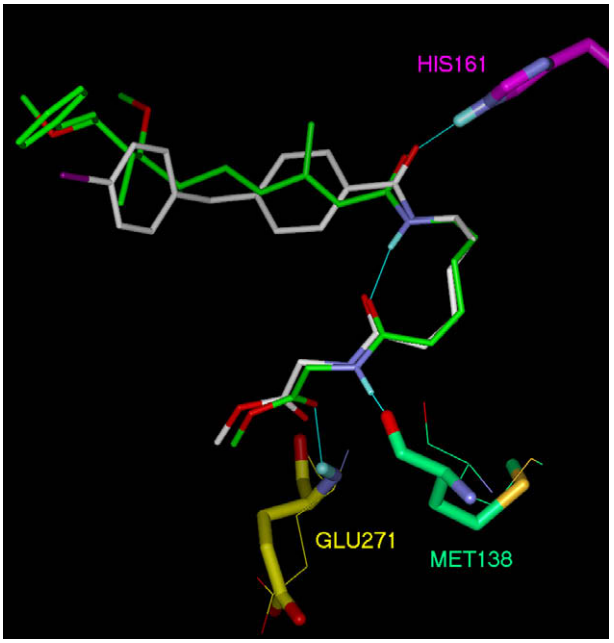

Figure 10. Superposition of the docked geometry of crocacin A **8** (green carbon atoms) on the crystallographically observed binding mode of compound **16** (white carbon atoms). The superposition was made by performing a least-squares fit of the C-α atoms of 25 binding site residues.

The binding site model, coupled with further molecular modeling, was used to design analogues of crocacins A and D, with mixed results. The fact that some of the designs were inactive, despite modeling well into the active site, highlights the limitations of a rather simple model based on shape fit, complementarity of hydrogen bonding groups, and ligand conformational analysis. Other important factors, such as solvation and entropic effects, were not considered and these can of course be critical in binding interactions. Nevertheless, the design strategy was successful in that analogues of the naturally occurring fungicide crocacin D were synthesized which were active both in a respiration assay, and also on fungi on plants, and which were significantly more stable than the natural compounds.

4. Methodology

4.1. Cytochrome *b* sequence comparisons

Fungal cytochrome *b* sequences were obtained from the UniProt Knowledgebase[31] for the following pathogens: *Puccinia triticina* (wheat brown rust, Q462L2); *Mycosphaerella graminicola*, (*Septoria tritici*, wheat glume blotch, A9Y5I4); and *Blumeria graminis f. sp. tritici* (wheat powdery mildew, Q9B335). The beef, chicken and yeast cytochrome *b* sequences were taken from the crystal structures (PDB IDs: 1sqx, 1bcc[19] and 1kyo[32]). The sequences were aligned using the MegAlign software[33] using the ClustalW multiple alignment method (with "Slow-Accurate" settings).

4.2. Molecular docking studies

A model of crocacin A was built within the Sybyl modeling package,[34] and energy-minimized using the MMFF4s force field.[25] This geometry was used as the initial conformation in the ligand docking work.

The Q_o site from the 1sqx structure was used for docking purposes, with the stigmatellin molecule removed. Hydrogen atoms were added in Sybyl, using the *biopolymer AddH* tool. The placement of hydrogen atoms on nearby side chain hydroxyl groups and histidine residues was carefully inspected, and the rotamers/tautomers adjusted where necessary to optimise the local hydrogen bonding of the residues concerned. When initial docking runs failed to give a plausible docking for crocacin A, the side chain of Glu272 was adjusted to orient it 'out' of the Q_o site, as found in other structures (1sqq and 1sqp).

Docking was performed using the GOLD software package (version 2.0) using the default ('slow standard') parameter settings, and the GoldScore fitness function. In addition to the standard settings, GOLD allows for various other options; for example internal hydrogen bonding may optionally be rewarded in the fitness function, and hydrogen bonding constraints can be added to ensure the docking solutions contain hydrogen bonds between specific groups in the protein and the ligand. A number of docking runs were performed to generate consensus solutions (as GOLD is a stochastic method, and the answers can vary from run to run) and also to explore the effects of rewarding internal hydrogen bonding in the ligand, and the effect of specifying protein-ligand hydrogen bonds (i.e. to His161 and Glu271).

4.3. Conformational analysis

Conformational analysis of model compounds containing the key substructural features of crocacin A was performed using the conformational searching tools in Sybyl, with the MMFF94s force field. In addition, the CSD was searched for molecules containing similar molecular fragments to those found in crocacin A and the rotameric preferences of these fragments were analyzed using the Vista program[35] for the analysis and display of data. The preferred dihedral angle values shown in Table 3 are those that are associated with low conformational strain energies (typically <1.5 kcal/mol per torsion angle, calculated using MMFF94s) or those that were significantly represented in the CSD searches.

4.4. Docking model refinement

High-ranking docking poses from the GOLD runs were compared with the results of the conformational analysis in the selection of a single preferred docking model. The Sybyl ANNEAL command was used, to energy-minimise the geometry of the docked crocacin A molecule, together with the surrounding Q_o site residues within a distance of 6 Å. The MMFF94s force field was used, and non-bonded interactions with residues up to 12Å from the bound ligand were included in the energy-minimization. The same method was also used in modeling the new ligand designs in the Q_o site.

5. Experimental

5.1. Glasshouse screening method

The compounds were diluted in reverse osmosis water to the desired final concentration immediately before use. Tween 20 (registered trade mark, at a final concentration of 0.05% by volume) was added with the water to improve retention of the spray deposit. The compounds were applied to the foliage of the test plants grown on an artificial, cellulose based growing medium, by spraying the plant to maximum droplet retention. Tests were carried out against *Mycosphaerella graminicola*, (*Septoria tritici*, wheat glume blotch), and *Puccinia triticina* (wheat brown rust) on wheat, *Plasmopara viticola* (vine downy mildew) on vine, and *Phytophthora infestans* (potato late blight) on tomato. Two replicates, each containing three plants were used for each treatment. The plants were inoculated with either a calibrated fungal spore suspension or a "dusting" with dry spores one day after chemical application. The plants were then incubated under high humidity conditions and put into an appropriate environment to allow infection to proceed until the disease was ready for assessment. The time period between chemical application and assessment varied from six to nine days according to the disease and environment. However, each individual disease was assessed after the same time period. The level of disease present (the percentage leaf area covered by actively sporulating disease) was assessed visually and the assessed values for all replicates were averaged to provide mean disease values. Compounds were tested at 100, 50, 25, 10, 5 and 1 ppm, and activity was defined as the breakpoint, that is, the lowest of the six concentrations at which 100% control of disease was achieved. This concentration was then converted into molar units. The standard azoxystrobin was tested at a concentration at which it gave 100% control over many tests.

5.2. NADH oxidase assay

The NADH oxidase assay was run as a microtitre plate assay. The test compound was dissolved and diluted in DMSO in a master plate. The compound was then transferred to the assay plate to give a final DMSO concentration of 2% and a final top concentration of test compound of 20 ppm. Mitochondria (purchased from Prof. P. Rich of University College, London), were added in pH 8.0 phosphate buffer, to a final mitochondria concentration of 68.8 μg/ml. The plate was incubated at room temperature for 15 min. The NADH substrate was added, in pH 8.0 phosphate buffer, to give a final NADH concentration of 200 ppm. The plate was read at 340 nm (absorbance) immediately and at six further times, at two minute intervals, and the IC_{50} computed. Each test sample was unreplicated. However, based on 64 separate IC_{50} estimates for a standard compound (azoxystrobin), the 95% confidence interval for a single result, R, is $R/4.3 - R \times 4.3$, and it is not unreasonable to assume that test samples will display similar (though not necessarily identical) levels of variation.

References and notes

1. Mitchell, P. *J. Theoret. Biol.* **1976**, *62*, 327.
2. Trumpower, B. L. *J.Biol.Chem.* **1990**, *265*, 11409.
3. Leroux, P.; Delorme, R. *Phytoma* **1997**, *494*, 17.
4. Ueki, M.; Machida, K.; Taniguchi, M. *Curr. Opin. Anti-Infect. Invest. Drugs* **2000**, *2*, 387.

5. Esser, L.; Quinn, B.; Li, Y.-F.; Zhang, M.; Elberry, M.; Yu, L.; Yu, C.-A.; Xia, D. *J. Mol. Biol.* **2004**, *341*, 281.
6. Gao, X.; Wen, X.; Esser, L.; Quinn, B.; Yu, L.; Yu, C. A.; Xia, D. *Biochemistry* **2003**, *42*, 9067.
7. von Jagow, G.; Link, T. A. *Methods Enzymol.* **1986**, *126*, 253.
8. Crofts, A. R.; Hong, S.; Ugulava, N.; Barquera, B.; Gennis, R.; Guergova-Kuras, M.; Berry, E. A. *Proc. Natl. Acad. Sci. U.S.A.* **1999**, *96*, 10021.
9. Pember, S. O.; Fleck, L. C.; Moberg, W. K.; Walker, M. P. *Arch. Biochem. Biophys.* **2005**, *435*, 280.
10. Gao, X.; Wen, X.; Yu, C.; Esser, L.; Tsao, S.; Quinn, B.; Zhang, L.; Yu, L.; Xia, D. *Biochemistry* **2002**, *41*, 11692.
11. Esser, L.; Gong, X.; Yang, S.; Yu, L.; Yu, C-A.; Xia, D. *PNAS* **2006**, *103*, 13045.
12. Höfle, H.; Kunze, B.; Jansen, R.; Reichenbach, H. *J. Antibiot.* **1994**, *47*, 881.
13. Beautement, K.; Clough, J. M.; de Fraine, P. J.; Godfrey, C. R. A. *Pest. Sci.* **1991**, *31*, 499.
14. Bartlett, D. W.; Clough, J. M.; Godwin, J. R.; Hall, A. A.; Hamer, M.; Parr-Dobrzanski, R. *Pest. Manag. Sci.* **2002**, *58*, 649.
15. Fisher, N.; Brown, A. C.; Sexton, G.; Cook, A.; Windass, J.; Meunier, B. *Eur. J. Biochem.* **2004**, *271*, 2264.
16. Smith, S. C.; Clark, E. D.; Ridley, S. M.; Bartlett, D.; Greenhow, D. T.; Glithro, H.; Klong, A. Y.; Mitchell, G.; Mullier, G. *Pest. Manag. Sci.* **2005**, *61*, 16.
17. Xia, D.; Yu, C. A.; Kim, H.; Xia, J. Z.; Kachurin, A. M.; Zhang, L. *Science* **1997**, *277*, 60.
18. Iwata, S.; Lee, J. W.; Okada, K.; Lee, J. K.; Iwata, M.; Rasmussen, B.; Link, T. A.; Ramaswamy, S.; Jap, B. K. *Science* **1998**, *281*, 64–71.
19. Zhang, Z.; Huang, L.; Shulmeister, V. M.; Chi, Y.-I.; Kim, K. K.; Hung, L.-W.; Crofts, A. R.; Berry, E. A.; Kim, S.-H. *Nature (London)* **1998**, *392*, 677.
20. Hunte, C.; Koepke, J.; Lange, C.; Rossmanith, T.; Michel, H. *Structure (London)* **2000**, *8*, 669.
21. Crofts, A. R.; Lee, S.; Crofts, S. B.; Cheng, J.; Rose, S. *Biochim. Biophys. Acta* **2006**, *1757*, 1019.
22. Hartshorn, M. J.; Verdonk, M. L.; Chessari, G.; Brewerton, S. C.; Mooij, W. T. M.; Mortenson, P. N.; Murray, C. W. *J. Med. Chem.* **2007**, *50*, 726.
23. Allen, F. H. *Acta Crystallogr.* **2002**, *B58*, 380.
24. Jansen, R.; Washausen, P.; Kunze, B.; Reichenbach, H.; Höfle, G. *Eur. J. Org. Chem.* **1999**, 1085.
25. Halgren, T. *J. Comp. Chem.* **1999**, *20*, 720.
26. Henrick, C. A. In *Agrochemicals from Natural Products*; Godfrey, C. R. A., Ed.; CRC Press, 1994; p 63.
27. Crowley, P. J.; Aspinall, I. H. C. R. A.; Devillers, I. M.; Munns, G.; Sageot, O.-A.; Swanborough, J.; Worthington, P. A.; Williams, J. *Chimia* **2003**, *57*, 685.
28. Godfrey, C. R. A.; Crowley, P. J.; Williams, J.; Swanborough, J. J.; Sageot, O. A. GB Patent 2380193, 2003; *Chem.Abstr.* **2003**, *138*, 271971.
29. Jones, G.; Willett, P.; Glen, R. C. *J. Mol. Biol.* **1995**, *245*, 43.
30. Daldal, F.; Dutton, P. L.; Gibney, B. R.; Saribas, A. S.; Valkova-Valchanova, M. B. *Biochemistry* **1998**, *37*, 16242.
31. The UniProt Knowledgebase. Available from: http://www.expasy.org/.
32. Lange, C.; Hunte, C. *Proc. Nat. Acad. Sci. U.S.A.* **2002**, *99*, 2800.
33. The MegAlign software is available from DNASTAR Inc., 1228 South Park Street, Madison, WI 53715, USA. Available from: http://www.dnastar.com/.
34. Sybyl is available from Tripos, 1699 South Hanley Road, St. Louis, MO 63144-2319, USA. (http://www.tripos.com).
35. Vista is available from the Cambridge Crystallographic Data Centre, 12 Union Road, Cambridge, UK. (http://www.ccdc.cam.ac.uk).